



Auxiliary ventilation in mining roadways driven with roadheaders: Validated CFD modelling of dust behaviour

J. Toraño *, S. Torno, M. Menéndez, M. Gent

Mining and Civil Works Research Group, School of Mines, Oviedo University, Asturias, Spain

ARTICLE INFO

Article history:

Received 23 March 2010
Received in revised form 26 July 2010
Accepted 30 July 2010
Available online 24 August 2010

Keywords:

Auxiliary ventilation
CFD modelling
Respirable dust
Coal mine

ABSTRACT

The production of dust when driving mining roadways can affect workers health. In addition, there is a decrease in productivity since Mine Safety regulations establish a reduction in the working time depending on the quartz content and dust concentration in the atmosphere.

One of the gate roadways of the longwall named E4-S, belonging to the underground coal mine Carbonar SA located in Northern Spain, is being driven by an AM50 roadheader machine. The mined coal has a high coal dust content.

This paper presents a study of dust behaviour in two auxiliary ventilation systems by Computational Fluid Dynamics (CFD) models, taking into account the influence of time. The accuracy of these CFD models was assessed by airflow velocity and respirable dust concentration measurements taken in six points of six roadway cross-sections of the mentioned operating coal mine.

It is concluded that these models predicted the airflow and dust behaviour at the working face, where the dust source is located, and in different roadways cross-sections behind the working face.

As a result, CFD models allow optimization of the auxiliary ventilation system used, avoiding the important deficiencies when it is calculated by conventional methods.

© 2010 Elsevier Ltd. All rights reserved.

1. Introduction

Dust generated by roadheaders, when advancing mining roadways, is a hazard to the health and safety of coal workers since they breathe polluted air causing pneumoconiosis. What is more, there is a decrease in productivity due to the fact that the Mine Safety regulations in Spain limit the presence of personnel at the work face by up to 66%, depending on the SiO₂ content of dust and concentration of respirable dust.

From the methods for dust control in underground mines, the water spraying is the simplest and the most widely used, reducing dust content in air by 50–60%, and with wet dust extractors the reduction can reach 99% (Toraño et al., 2004; Mikki, 2005).

The use of these methods helps to clean the air, but the greatest contributing factor, to keep safe conditions of those working underground, is the quality of the auxiliary ventilation system at the working face (Colinet et al., 1991; Kissell, 2003). The quality is achieved by the correct choice of the auxiliary ventilation system.

Studies conducted by Kissell and Wallhagen (1976), Haney et al. (1982) and Schultz et al. (1993) proved that the face ventilation effectiveness (FVE), or proportion of fresh air reaching the working

face, is 39.9% for a forcing ventilation system, whereas it is 10% for an exhausting ventilation system.

Studies made by this research group, Toraño et al. (2009), indicate FVE values of 35% and 12% respectively and that 10 m is the distance of the ductwork from the face that produces the lowest percentages of dead zones, that is to say, roadways zones with velocities lower than 0.2 m/s.

Taking into account the studies mentioned above and that the pollutant here is dust, a forcing auxiliary ventilation system together with an exhausting one were chosen. This allows the correct displacement, capture and dilution of dust.

Capturing dust from the face, through the exhausting ventilation system, permits bringing the forcing duct closer to the face, displacing dust produced at the face in a better way.

When the problem of pollutant dilution, gases or dust, is analysed by conventional methods, it gives deficient results, due to the fact that airflow and pressure values are defined for a specific point of a determined cross-section at a fixed instant (Onder and Cevik, 2008; Suglo and Frimpong, 2001; Toraño et al., 2002).

It is necessary to analyse the problem by Computational Fluid Dynamics (CFD3D), bearing in mind the influence of time on the auxiliary ventilation system, and to validate these prediction models with a series of underground measurements (Srinivasa et al., 1993; Heerden and Sullivan, 1993; Moloney et al., 1999a; Parra et al., 2005; Uchino and Inoue, 1997; Wala et al., 2003).

* Corresponding author. Address: Independencia 13, 33005 Oviedo, Asturias, Spain. Tel.: +34 985104254; fax: +34 985104245.

E-mail address: jta@uniovi.es (J. Toraño).

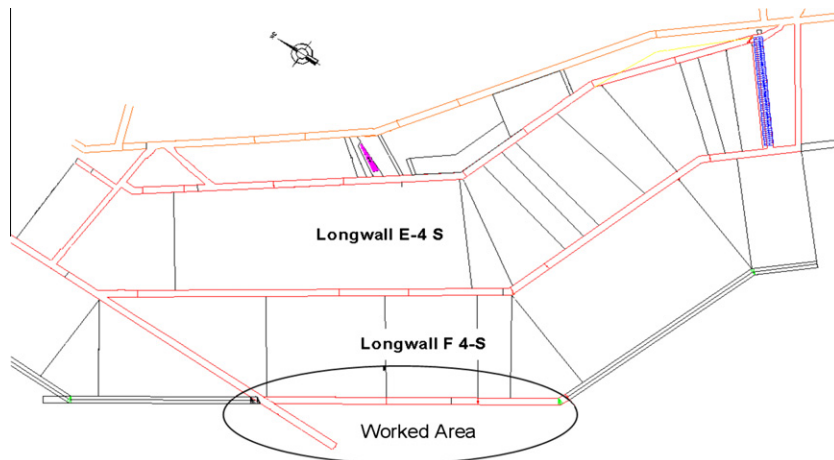


Fig. 1. Layout of the worked area.

The aim of this paper is to prove that the mentioned CFD models allow firstly, to choose the more appropriate auxiliary ventilation system, secondly, to obtain in a continuous way how airflow and dust develop along the roadway, and thirdly, their influence on the working face workers. Furthermore, these models permit to know how the different positions of the ductworks in the roadway and the airflow provided by the fans affect to the previous one.

Field measurements, airflow velocity and dust concentration, were taken in the gate roadway of the longwall named E4-S of the mentioned underground mine. In order to validate the predicted CFD results, it was considered very important to take measurements in an operating underground coal mine in real situations.

2. Underground airflow and dust measurements

Carbonar mine is located in Rengos coal basin, in Asturias, Northern Spain, which has a very important mining tradition. At present the mine is working a coalbed named “Capa Ancha” at a depth from surface of 550 m. The coalbed is 4 m thick and 14–26° deep. A layout of the mine with the studied zone can be seen in Fig. 1.

The powered support consists of 53 two leg lemniscate shield support Glinik 18/41 Poz, with a height range from 1.80 to 4.10 m. The coal mining machine is a bidirectional double drum shearer loader Famur KGS-324, with 2×132 kW cutting power, and the face conveyor is Glinik 260/724 BP1 with a maximum carrying capacity up to 1000 tonnes per hour, (Toraño et al., 2003).

The gate roadways were driven with an arched-section of 14.7 m^2 (5.0 m wide and 3.70 m high), using yielding steel sets of

29 kg/m, TH profile. These steel sets, named CB1000, have a spacing of 1.00 m. These roadways are 1000 m in length and they are advanced 6 m/day by an Alpine AM50 roadheader of 155 kW in two shifts.

The granulometric composition of the mined coal was determined by laser Coulter analysis (Particle Size Analyzer) in the INCAR (National Coal Institute belonging to the CSIC-Spanish Council for Scientific Research) and it indicated a high content of coal dust, 1.75%, which is equivalent to 17.5 kg per tonne.

From the different auxiliary ventilation systems that can be used, the two systems which have given better results will be analysed.

One consists of a 300 mm diameter forcing duct, located 3 m from the face, with an airflow of $1.5 \text{ m}^3/\text{s}$ and an exhausting duct of 600 mm in diameter located 6 m from the face, with an exhausted airflow of $6.5 \text{ m}^3/\text{s}$. Both ducts, forcing and exhausting, are hung from the roadway roof. This auxiliary ventilation system will be called E-R below.

The other auxiliary ventilation system is similar to the previous one, but with the exhausting duct located on the roadway floor. This auxiliary ventilation system will be called E-F below.

Fig. 2 shows the AM50 roadheader driving the roadway in a 4.0 m thick coalbed with details of the ripping cutting head and the exhausting duct of the E-R auxiliary ventilation system. Fig. 3 illustrates the geometric model of the mentioned E-R ventilation system.

Miniair Junior Macro-MIE hand-held anemometers (range of 0–20 m/s with an error of 1%) were used to measure airflow velocities. A HD-1004 Haz-Dust IV collector, whose specifications are



Fig. 2. AM50 roadheader driving the roadway in the coalbed.

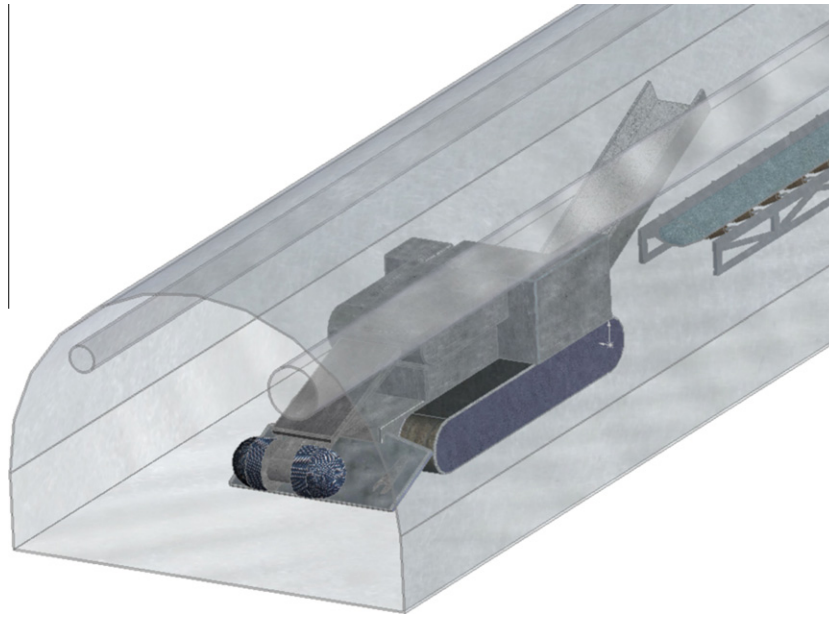


Fig. 3. 3D modelling of the AM50 roadheader and the auxiliary E-R ventilation system.

depicted in Table 1, and GT640 Met One dust collectors, whose specifications are shown in Table 2, were used for measuring respirable dust concentrations. Fig. 4 shows the Haz-Dust IV and Met One dust collectors in operation.

The microscopic analyses of respirable dust, taken from the dust collectors was conducted with a Zeiss Axioplan optical microscope linked up to Leica software for capturing images. Coal of this coal-field has a very low quartz content. Fig. 5 shows a microphotograph of respirable dust where a particle containing pyrite can be seen.

Airflow velocity and dust concentration measurements, in six points of six cross-sections at 0, 0.5, 3, 6, 12 and 24 m respectively from the face, were taken. Distribution of these six points is presented in Fig. 6 for the E-F model as an example. Points 4 and 5 were located in a horizontal plane at 0.5 m from the floor; points 2, 3 and 6 were located in a horizontal plane at 1.8 m from the floor, and point 1 at 0.5 m from the roof.

On average, the advance achieved per shift by the roadheader is 3 m with cutting cycles of 1 m at which steel sets are placed.

Table 1
Haz-Dust IV specifications.

Specification	Range
Accuracy	±10% NIOSH 0600 with SAE test dust
Precision	0.02 mg/m ³
Sensing range	0–200 mg/m ³
Particle size range	0.1–10 µm respirable 0.1–50 µm thoracic 0.1–100 µm inhalable (IOM)
Recording time	1 s, 1 min and 10 min averages

Table 2
Met One specifications.

Specification	Range
Accuracy	±8% of Niosh 0600
Precision	0.003 mg/m ³
Sensing range	0–100 mg/m ³
Particle size range	0.1–100 µm
Recording time	1 s

In each one of the cutting cycles dust concentration and airflow velocity measurements are taken in two points, in such a way that, in each shift, airflow velocity and dust concentration measurements are carried out in six points, that is to say, in a roadway cross-section.

In each point the average of 10 airflow velocity measurements were taken and for dust concentrations continuous measurements were carried out at minute intervals for 20 min.

For two daily shifts, measurements were carried out in two cross-sections per day, which means that, for the 30 work days, 15 measurements, for each roadway cross-section studied at 0 m, 0.5 m, 3 m, 6 m, 12 m and 24 m from the working face, were obtained.

The total number of airflow velocity measurements were 1800 and the total number of dust concentration measurements were 3600. To obtain these experimental data was complex due to the fact that the mine was in operation (for example the different roadheader movements), collecting data only in the presence of the machine operator and a researcher. Meanwhile, auxiliary operations behind the machine were stopped so as not to interfere in both the airflow and the dust concentration measurements. The complexity of the location of point 1, placed on the roadway roof, is significant.

Fig. 7 shows the evolution of dust concentrations obtained, during 20 min, by the Met One GT640 dust collector at point 6, for a cross-section located 0.5 m from the working face and for the two auxiliary ventilation systems.

Correlations between the experimental airflow velocity measurements and those obtained by CFD modelling are shown in Section 3 and correlations between the experimental dust concentration measurements and those predicted by CFD modelling are shown in Section 5.

3. Auxiliary ventilation behaviour by CFD modelling

In this paper two different geometries, according to the location of the exhausting duct and maintaining the same computational characteristics, are taken into account. The computational domain consists of a CB1000 roadway with two auxiliary ventilation ducts with a diameter of 300 and 600 mm, corresponding to forcing and

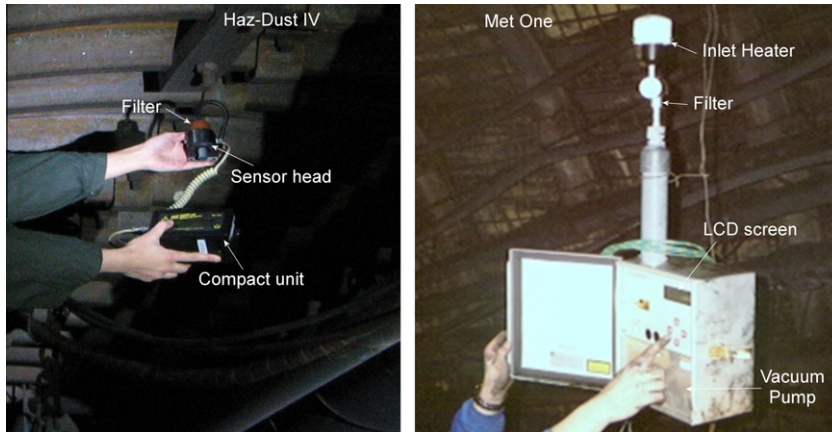


Fig. 4. Haz-Dust IV and Met One dust collectors working.

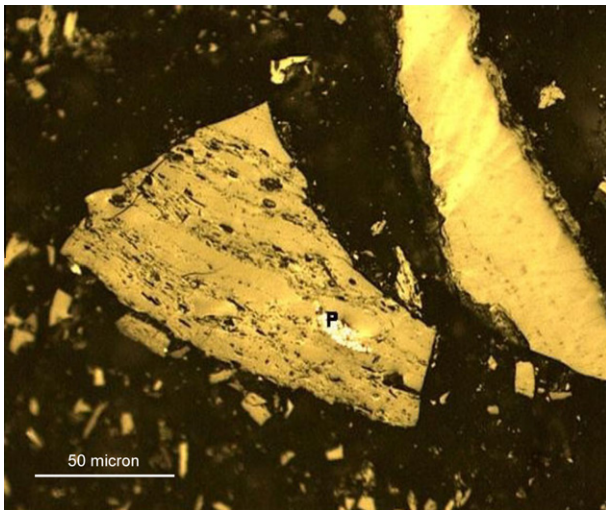


Fig. 5. Coal particle containing pyrite.

exhausting system respectively and an Alpine Miner AM50 roadheader; all of it created by SolidWorks (2004) software (Computer-aided geometric modelling).

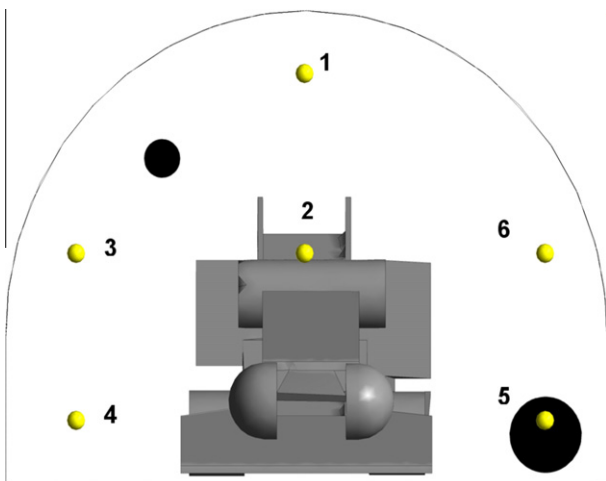


Fig. 6. Roadheader and fixed-point measurements across cross-sections for the auxiliary E-F ventilation system.

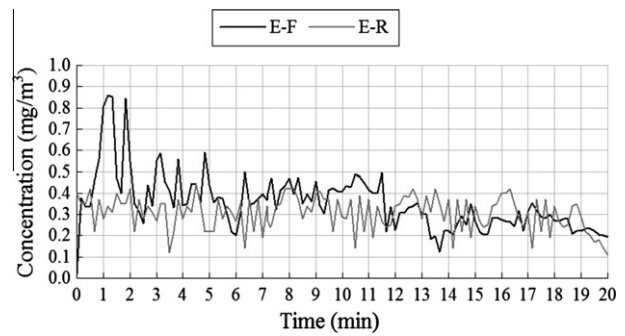


Fig. 7. Evolution dust concentrations at point 6, cross-section 0.5 m for the E-R and E-F systems.

This geometry is divided into control volumes where the partial differential equations are solved iteratively. The discretisation of the model is carried out in the IcemCFD 10.0, achieving a meshing of 1300,000 elements, an adequate value for these simulations according to grid independence studies which have been carried out by this research group in other tunnel ventilation studies, (Torano et al., 2006a, 2009). In the boundary layer, where a high resolution of calculation is required, a finer meshing with elements ten times smaller and orientated to the flow direction was obtained. The mesh quality is sufficiently high so that the calculations are independent to the used mesh.

In Fig. 8 the geometry and the tetrahedron meshing of the computational model, where the green elements indicate a high quality and the yellow ones a lower quality, are shown.

The Computational Fluid Dynamics Ansys CFX 10.0 commercial software was used to model the multiphase flow behaviour (air-particles) in underground roadways with a roadheader operating.

Ansys CFX uses the Finite Volume Method to calculate the Navier–Stokes equations (Ansys CFX, 2009a) which describe the processes of momentum, heat and mass transfer, Eqs. (1)–(3). This method divides the region of interest into small control volumes, where the Navier–Stokes equations are discretised and solved iteratively.

$$\rho \frac{D\bar{V}}{Dt} = -\bar{\nabla}p + \rho\bar{g} + \mu\nabla^2\bar{V} \tag{1}$$

$$\frac{D\rho}{Dt} + \rho\bar{\nabla} \cdot \bar{V} = 0 \tag{2}$$

$$\rho \frac{Dh}{Dt} = K\nabla^2T - p\bar{\nabla} \cdot \bar{V} \tag{3}$$

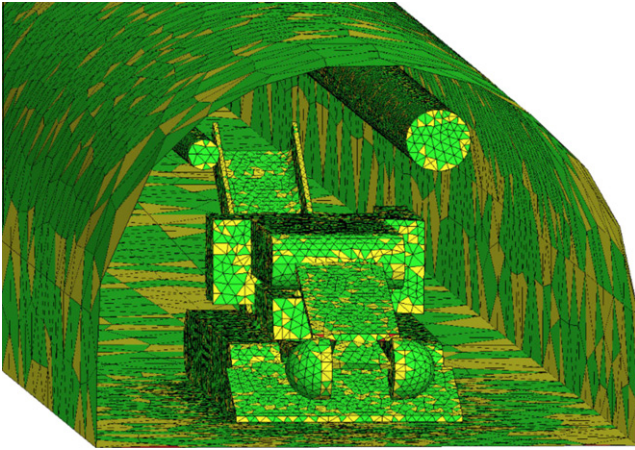


Fig. 8. Geometry and model meshing for the E-R auxiliary ventilation system.

where ρ is the density, ∇ is the operator divergence, ∇ is the gradient, μ is the viscosity, T is the temperature, t is the time, V is the velocity, h is the specific enthalpy and K is the conductivity.

Turbulence closure model is reached by means of the Standard k-epsilon turbulence model. The choice of this turbulence model is based on a comparative study between experimental and CFD data for different turbulence models, such as Spalart Allmaras, k-omega, Standard k-epsilon and SST, (Torano et al., 2006b, 2009).

Recent studies with turbulent flows in cyclones (Gupta et al., 2008) have taken more complex turbulence models into account (RNG k-epsilon model and BSL Reynolds Stress model) which were added to the latter comparative study.

The comparative results by means of the results of the linear regression (r^2 parameter), that is, the relationship between CFD values and field measurement values, for each turbulence model, are shown in Fig. 9. The Standard k-epsilon model provides better results when compared with experimental measurements. Other authors such as Norton et al. (2007), Ballesteros-Tajadura et al. (2006), Moloney et al. (1999a), Moloney and Lowndes (1999b) and Hargreaves and Lowndes (2007) have also used the k-epsilon turbulence model to simulate the roadway flow obtaining valid results. Zhang and Chen (2006) have also obtained valid results with k-epsilon models when they have studied pollutant dust dispersion in ventilated rooms.

The computational domain is characterized by a flow (air) at 25 °C and it is affected by the gravity.

The CFD modelling consists of three different boundary conditions, Inlet, Opening and Wall. The inlet is at the forcing duct outlet with airflow of 1.5 m³/s. The opening corresponds to both the exhausting duct with an airflow of 6.5 m³/s and the roadway exit.

The remaining model surfaces are walls characterized for being free-slip except the roadway wall, the working face and the floor which have roughness of 5 cm. The particle injection is carried out uniformly from the working face.

The particle movement is described by means of the Lagrangian Particle Tracking multiphase model (Ansys CFX 12.0, 2009a,b). The Particle Transport Model models the dispersed phase (particles) which is discretely distributed in the continuous phase (air), which implies a separated calculation for each phase with source terms of the particle effects for the continuous phase.

The separated flow analysis model is implemented in the Lagrangian Particle Tracking model to characterize the dispersed phase behaviour, which is represented by track where each particle represents a sample of particles that follow an identical path. For this study the coupling between the phases is a one-way coupling, where the flow affects the particles but the particles do not affect the flow.

The Lagrangian or Particle Tracking model implemented in Computational Fluid Dynamics is based on calculating the equation of a particle trajectory, taking into account variables such as velocity and density.

The particle displacement is calculated by Eq. (4):

$$x_i^n = x_i^0 + v_{pi}^0 \delta t \tag{4}$$

where the superscripts 0 and n refer to old and new values respectively, v_{pi}^0 is the particle velocity and δt is the Euler integration of particle velocity over time step.

The particle velocity is calculated by using the following equations:

$$v_p = v_f + (v_p^0 - v_f) \exp\left(-\frac{\delta t}{\tau}\right) + \tau F_{all} \left[1 - \exp\left(-\frac{\delta t}{\tau}\right)\right] \tag{5}$$

where

$$\tau = \frac{4d\rho_p}{3\rho_f C_D} |v_f - v_p| \tag{6}$$

d is the diameter of the particle, v_p the velocity of the particle and v_f the fluid velocity.

The movement equation (equation of the movement quantity momentum), for a particle in flows where the density of the particle is greater than the fluid density, is simplified into:

$$m_p \frac{dv_p}{dt} = \underbrace{\frac{1}{8} \pi \rho_f d^2 C_D |v_f - v_p| (v_f - v_p)}_{\text{Drag Force over the Particles}} + F_b - \underbrace{\frac{\pi d^3}{6} (\rho_p - \rho_f) \omega \times (\omega \times R \varpi)}_{\text{Centripetal Force}} - \underbrace{\frac{\pi d^3 \rho_p}{3} \omega \times v_p}_{\text{Coriolis's Force}} \tag{7}$$

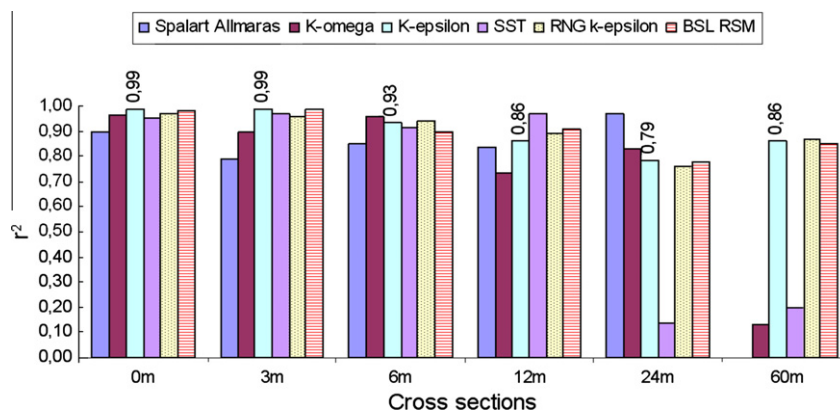


Fig. 9. Coefficient r^2 values for 6 turbulence models and six cross-sections.

where m_p is the particle mass, t is the time, d is the particle diameter, ρ_f is the fluid density, ρ_p is the particle density, R is the rotation radius vector, F_b is the floating force due to gravity, ω is the rotational velocity and C_D is the dragging coefficient.

The simulation calculations are carried out by means of iterations reaching a possible solution when the convergence is reached. This convergence is considered to be appropriate, when according to Ansys CFX (2009a), a value of 10^{-5} is achieved.

4. CFD modelling of airflow behaviour

Fig. 10 shows the 3D k-epsilon models of the two tested auxiliary ventilation systems: E-R (a) and E-F (b). For the mentioned ventilation systems in Figs. 11 and 12 a plane of velocity vectors situated 1 m from the floor and a plane of velocity vectors parallel to the floor at the height of point 2 (1.8 m), are shown.

It can be seen in Fig. 10b how the forcing ventilation streamlines remove particles from the working face, reaching maximum velocities in the lower left roadway corner where the exhausting duct is located.

Considering that the airflow with negative velocities goes towards the face and the airflow with positive velocities goes towards the roadway, for the E-F ventilation system and for a plane at 1 m from the floor, the airflow moves towards the face with velocities between -0.72 and -0.11 m/s and it comes back on both sides of the roadheader towards the roadway. The highest velocities are reached on the side where the exhausting duct is

placed, $+2.5$ m/s; on the other side of the roadheader, velocities are between 0 and $+1.14$ m/s.

For the E-R ventilation system and for a plane at 1 m from the floor, the airflow moves with velocities between -0.89 and 0.15 m/s and it comes back on both sides of the roadheader towards the roadway. The highest velocities are reached on the side where the exhausting duct is placed, $+1.83$ m/s, being the velocities about 0.5 m/s on the other side of the roadheader.

Figs. 11 and 12 show the distribution of velocity vectors produced in the vicinity of the roadheader and it can be observed how the turbulence is greater at the mid-height of the roadway (1.8 m).

Fig. 13 illustrates the evolution of airflow velocities going from the working face and along the roadway.

Fig. 14 shows, as an example, velocity isocontours in a roadway cross-section located 6 m from the face.

Maximum velocities, Fig. 13a, are similar for the two auxiliary ventilation systems, with the highest maximum velocity taking place at 6 m from the face with values of 21 m/s due to the turbulence and the nearby exhausting duct.

Average velocities, Fig. 13b, are higher for the E-F ventilation, with the highest average velocity at 6 m from the face, with values of 0.79 m/s. It can be seen that dead zones, or areas with velocities lower than 0.2 m/s, are produced at about 1.5 m and 3 m from the face.

These lower airflow velocity zones may be dangerous since gases and dust accumulate in them.

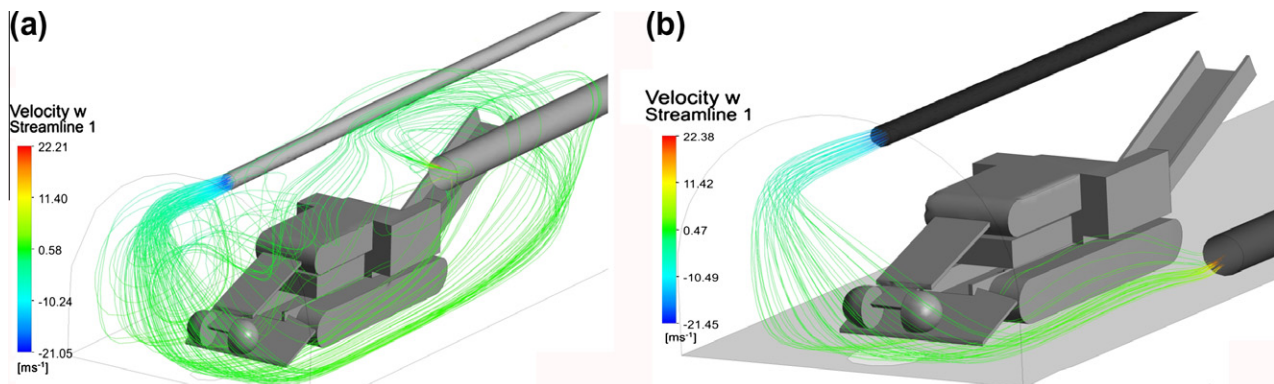


Fig. 10. Velocity distribution according to airflow streamlines.

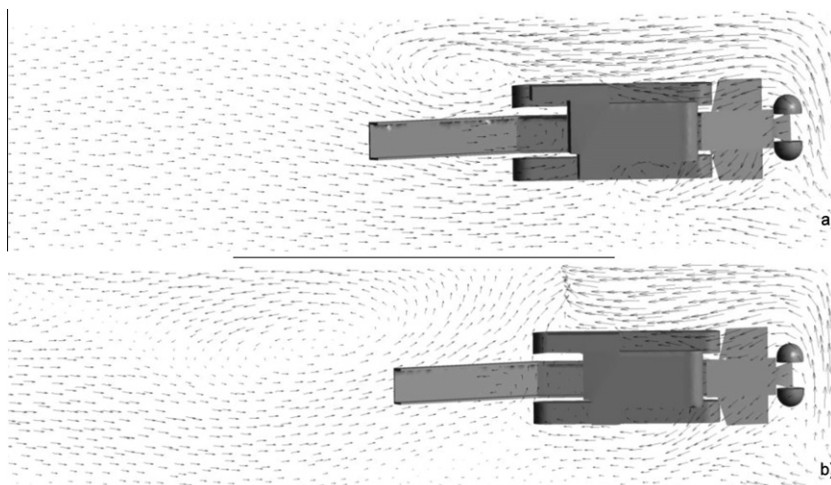


Fig. 11. Velocity vectors for a plane parallel to the floor at 1 m from it.

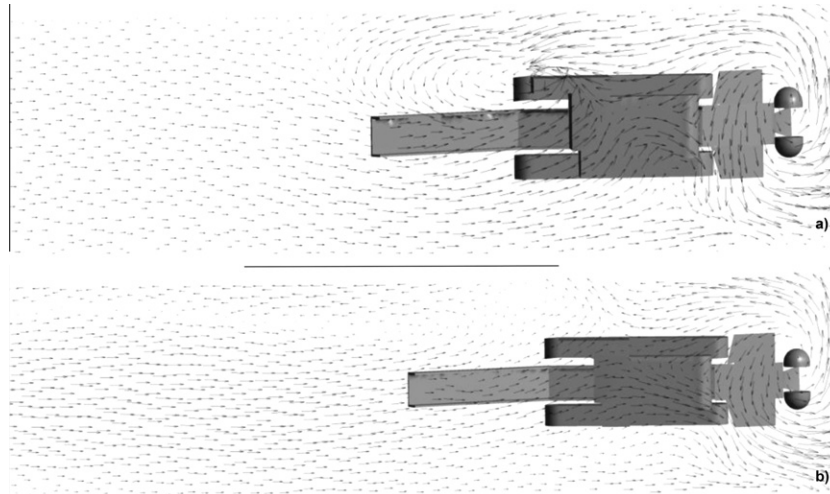


Fig. 12. Velocity vectors for a plane parallel to the floor at a height of point 2 (1.8 m).

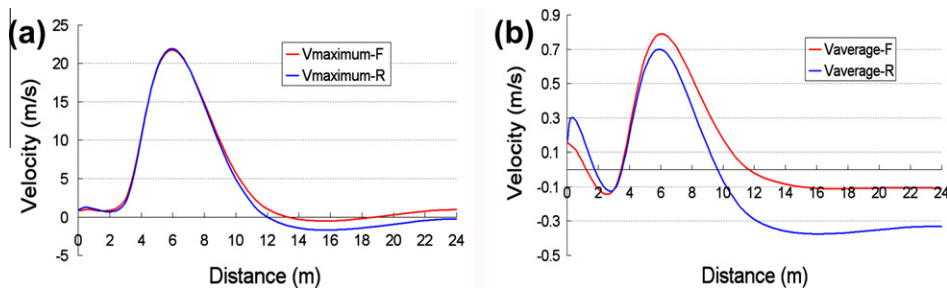


Fig. 13. Evolution of maximum and average velocities along the roadway.

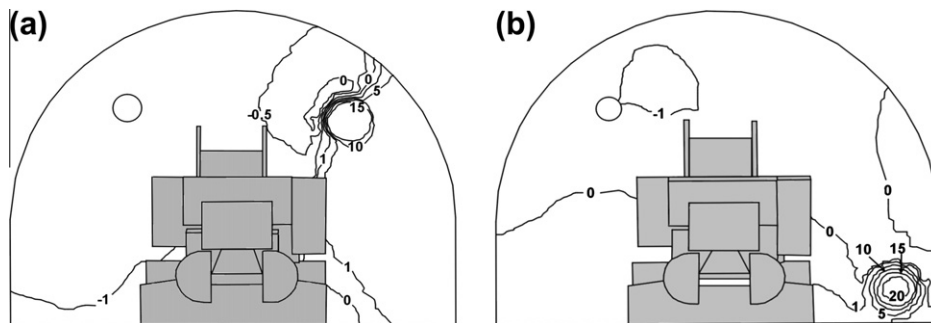


Fig. 14. Velocity isocontours of a cross-section located 6 m from the face.

5. CFD modelling of dust behaviour

Fig. 15a shows the evolution, along the roadway, of maximum values of dust concentrations measured into the mine and those predicted by CFD.

Fig. 15b shows the evolution, in each cross-section along the roadway, of average values of dust concentrations measured into the mine and those predicted by CFD.

Fig. 16 illustrates, as an example, dust concentration isocontours in a roadway cross-section located 0.5 m from the working face.

The evolution of maximum dust concentrations, Fig. 15a, presents higher values for the E-R ventilation system, with a maxi-

imum of 7.7 mg/m³ in some roadway points at 3 m from the face. For the E-F ventilation system the maximum value is 4.6 mg/m³.

For a cross-section at 0.5 m from the face, there are roadway points where the maximum dust concentration is 2.44 mg/m³ for the E-R system and 2.15 mg/m³ for the E-F system.

For both auxiliary ventilation systems the average dust concentrations, Fig. 15b, go from 0.43 mg/m³ in cross-sections near the working face to almost null values in cross-sections at 12 m from the face.

The evolution of average dust concentrations presents lower values for the E-F ventilation system. This is due to the fact that, although at the face the dust displacement mechanism is similar for the two ventilation systems, between the face and the cross-

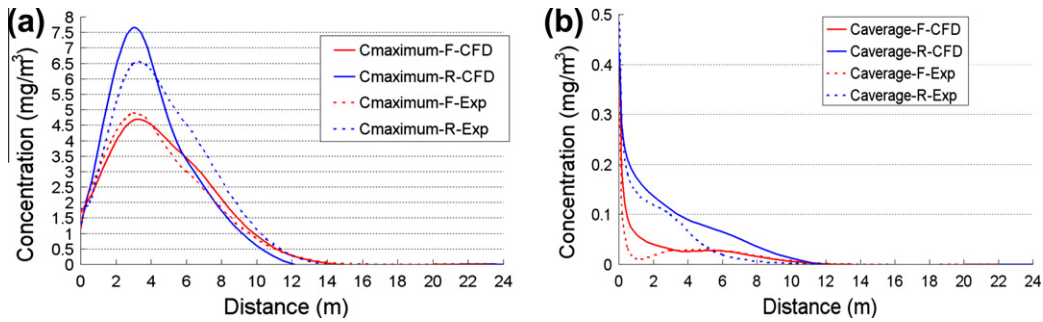


Fig. 15. Maximum and average experimental and CFD concentrations along the roadway.

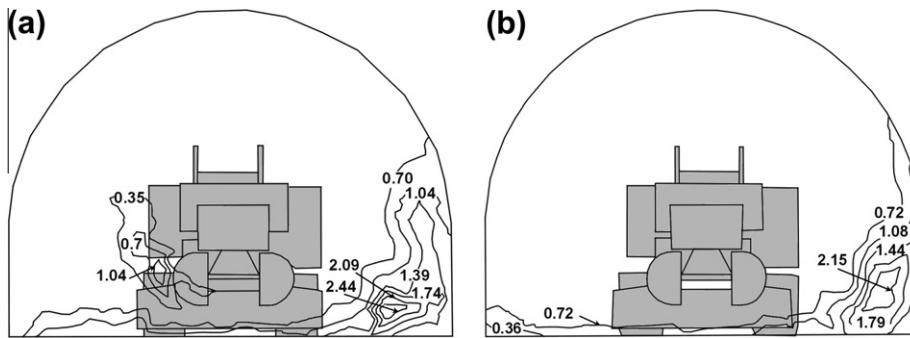


Fig. 16. Concentration isocontours in mg/m^3 of a cross-section located 0.5 m from the face.

section located 3 m from it, the dust displacement mechanism is more efficient with the E-F ventilation system.

From the mentioned cross-section, 3 m from the face, dust is captured and diluted and the E-R ventilation system presents higher dust concentration values.

Threshold limit values (TLV), based on recommendations of the American Conference of Governmental Industrial Hygienists and the Federal Mine Safety and Health Act of 1977, mandate that coal mine dust levels be below $2 \text{ mg}/\text{m}^3$ for a working shift. When quartz particles are present in the coal dust, additional restrictions are applied (McPherson, 1993; Vinson et al., 2007).

In Fig. 15b it can be seen that average dust concentration values in each roadway cross-section are lower than $2 \text{ mg}/\text{m}^3$. However, for the maximum values, there are some roadway cross-sections where, in certain points, dust concentration values are higher than $2 \text{ mg}/\text{m}^3$.

For the maximum value of $7.7 \text{ mg}/\text{m}^3$, corresponding to certain points of the roadway cross-section at 3 m from the working face, not only there would be health problems but also less productivity since Spanish Regulations (ASM-2, 1985) mandate a reduction in the time of dust exposure and hence in the working time. This

working time reduction could be up to 80% depending on the quartz content in dust.

Taking into account all of the above and due to the presence of the roadheader operator, it is important to carry out the analysis of the evolution of dust concentration and airflow velocity in point 2 along the roadway.

Fig. 17 shows the mentioned evolution of experimental values, measured in the mine, and those values obtained by CFD modelling. A good correlation can be observed between the measured and predicted results for airflow velocities and dust concentrations.

The E-F auxiliary ventilation system presents lower dust concentration in the 6 first metres of the roadways, as a result of the higher airflow velocities in that zone.

From the face to the cross-section located 1 m from it there is a considerable increase in airflow velocity which leads to, by means of the displacement mechanism, an important initial drop in dust concentration.

Later, although airflow velocity decreases as far as the roadway cross-section located 3 m from the face, dust concentration goes on decreasing due to dust capture by the exhausting ventilation.

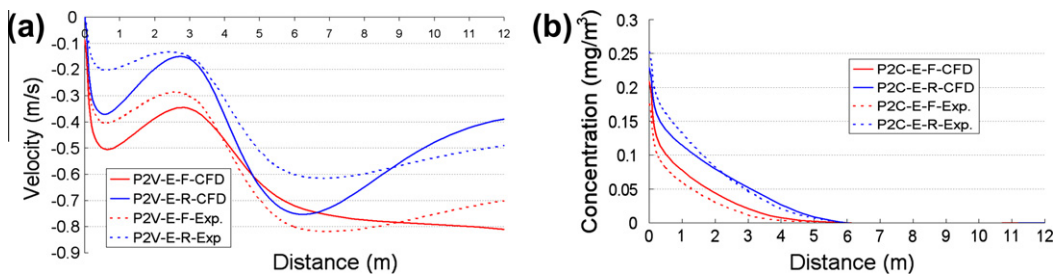


Fig. 17. Evolution of airflow velocities and dust concentrations for point 2.

Fig. 18 illustrates, for the two auxiliary ventilation systems, dust isoconcentrations in mg/m^3 for a plane parallel to the roadway floor at a height of 0.4 m, that is to say, at the height of points 4 and 5.

It can be observed, for the E-R ventilation system, some zones where there are high dust concentration values in the rear of the roadheader and in the near vicinity of the roadheader operator. Some of these values are below statutory levels but other values are above them.

Fig. 19 shows, for the two auxiliary ventilation systems, dust isoconcentrations in mg/m^3 for a plane parallel to the roadway

floor at a height of 3 m, that is to say, at the height of point 2, in a zone close to the face. It can be observed that, although dust concentration values are a bit higher for the E-R ventilation system, those concentrations are below statutory levels.

Fig. 20 shows, for the two auxiliary ventilation systems, dust isoconcentrations in mg/m^3 in a $2\text{ m} \times 2\text{ m}$ section close to the face in a longitudinal plane following the roadway axis. Besides high dust concentration values at the working face for the two ventilation systems, for the E-R system high dust concentration values are also produced in the zone of the roadheader loading apron and in the near vicinity of the machine operator.

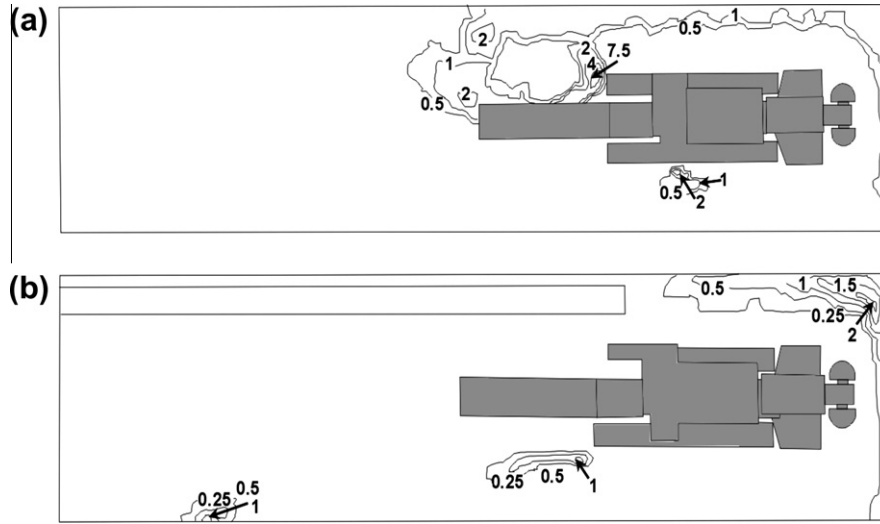


Fig. 18. Dust isoconcentrations (mg/m^3) for a plane parallel to the floor at a height of points 4 and 5 for both ventilation systems.

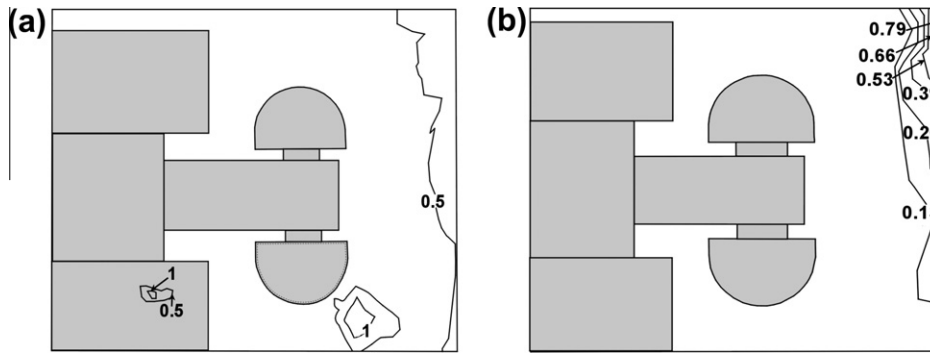


Fig. 19. Dust isoconcentrations for a plane parallel to the roadway floor at a height of point 3 for both ventilation systems.

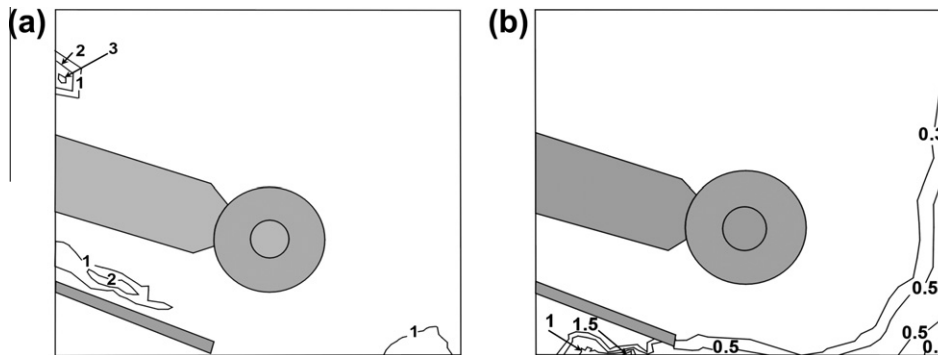


Fig. 20. Dust isoconcentrations (mg/m^3) for a longitudinal plane following the roadway axis for both ventilation systems E-R and E-F.

6. Conclusions

The aim of this work was to demonstrate the necessity of analysing dust behaviour in auxiliary ventilation systems by computational fluids dynamics. Field measurements were taken in an operating coal mine in order to validate these CFD models.

CFD models predict dust evolution in the roadway and therefore those cross-sections in which, although average dust concentration values are below statutory levels, there are high dust concentration values which are above statutory levels in some points of the mentioned cross-sections.

It is concluded that these predictive models allow to modify auxiliary ventilation and thus to improve health conditions and productivity. The most effective modifications were to increase air-flow velocity in the ducts, both forcing and exhausting, to modify the distance of those ducts from the face, to modify the height of the exhausting duct from the floor and to reinforce ventilation by additional systems.

It is necessary to monitor dust concentration and airflow velocity measurements in order to validate CFD models in a continuous manner. Based on such measurements and modelling it is possible to predict dust behaviour when its quantity varies as a result of an increase in daily advance of the roadheader or when the mined coal characteristics change.

Acknowledgements

This research work has been conducted by the Mining and Civil Works Research Group of the Oviedo University in collaboration with Carbonar S.A. Company.

The authors are grateful to Carbonar S.A. Mining Company for the access to their underground mines and for financing this study (Research Project CN-10-005).

References

- Ansys CFX-Solver, 2009a. Release 12.0: Modelling. Theory, pp. 241–262.
- Ansys CFX-Solver, 2009b. Release 12.0: Modelling. Particle Transport Modelling, pp. 195–240.
- ASM-2 (04.8.02), 1985. RGNBSM Standard. Labores subterráneas. Ventilación y desagüe: lucha contra el polvo.
- Ballesteros-Tajadura, R., Santolaria-Morros, C., Blanco-Marigorta, E., 2006. Influence of the slope in the ventilation semi-transversal system of an urban tunnel. *Tunn. Undergr. Space Technol.* 21, 21–28.
- Colinet, J.F., McClelland, J.J., Jankowski, R.A., 1991. Interactions and Limitations of Primary Dust Control for Continuous Miners. Bureau of Mines, RI 9373. NTIS No. PB91-241257. US Department of the Interior, Pittsburgh, PA.
- Dassault Systemes SolidWorks Corp., 2004. Velizy, France.
- Gupta, R., Kaulaskar, M.D., Kumar, V., Sripriya, R., Meikap, B.C., Chakraborty, S., 2008. Studies on the understanding mechanism of air core and vortex formation in a hydrocyclone. *Chem. Eng. J.* 144, 153–166.
- Haney, R.A., Gigliotti, S.J., Banfield, J.L., 1982. Face ventilation systems performance in low-height coal seams. In: *Proceedings of the First Mine Ventilation Symposium*, vol. 7, p. 8.
- Hargreaves, D.M., Lowndes, I.S., 2007. The computational modeling of the ventilation flows within a rapid development drive. *Tunn. Undergr. Space Technol.* 22, 150–160.
- Heerden, J., Sullivan, P., 1993. The application of CFD for evaluation of dust suppression and auxiliary ventilation systems used with continuous miners. In: *Proceedings of the 6th US Mine Ventilation Symposium*, pp. 293–297.
- Kissell, F.N., Wallhagen, R.E., 1976. Some new approaches to improve ventilation of the working face. In: *Proceeding of the NCA/BCR Coal Conference*, pp. 325–338.
- Kissell, F.N., 2003. *Handbook for Dust Control in Mining*. US Department of Health and Human Services. Public Health Service, Centers for Disease Control and Prevention. National Institute for Occupational Safety and Health, Pittsburgh Research Laboratory.
- McPherson, M.J., 1993. *Subsurface Ventilation Engineering*. Part 5. Dust. Mine, Ventilation Services, Inc. pp. 1–40.
- Mikki, P., 2005. Recent developments in dust control for mining and tunnelling operations. *Glückauf* 1, 23–27.
- Moloney, K.W., Lowndes, I.S., Hargreaves, D.M., 1999a. Analysis of flow patterns in drivages with auxiliary ventilation. *Trans. Inst. Min. Metall. (Sec. A: Min. Ind.)* 108, 17–26.
- Moloney, K.W., Lowndes, I.S., 1999b. Comparison of measured underground air velocities and air flows simulated by computational fluid dynamics. *Trans. Inst. Min. Metall. (Sec. A: Min. Ind.)* 108, 105–114.
- Norton, T., Sun, D-W., Grant, J., Fallon, R., Dodd, V., 2007. Applications of computational fluid dynamics (CFD) in the modelling and design of ventilation systems in the agricultural industry. *Bioresour. Technol.* 98, 2386–2414.
- Onder, M., Cevik, E., 2008. Statistical model for the volume rate reaching the end of ventilation duct. *Tunn. Undergr. Space Technol.* 23, 179–184.
- Parra, M.T., Villafruela, J.M., Castro, F., Méndez, C., 2005. Numerical and experimental analysis of different ventilation systems in deep mines. *Build. Environ.* 41, 87–93.
- Schultz, M.J., Beiter, D.A., Watkins, T.R., Baran, J.N., 1993. *Face Ventilation Investigation*. Clark Elkorn Coal Company. Pittsburgh Safety and Health Technology Center, Ventilation Division, Investigative Report No. P385-V286.
- Srinivasa, R.B., Baafi, E.Y., Aziz, N.I., Singh, R.N., 1993. Three dimensional modeling of air velocities and dust control techniques in a longwall face. In: *Proceedings of the 6th US Mine Ventilation Symposium*, pp. 287–292.
- Suglo, R.S., Frimpong, S., 2001. Assessment of the efficiencies of auxiliary ventilation systems using empirical methods. *Can. Inst. Min. Metall. Bull.*, 67–71.
- Toraño, J., Rodríguez, R., Cuesta, A., Diego, I., 2002. A computer program for calculating ventilation in tunnelling works based on an explicit method. *Tunn. Undergr. Space Technol.* 17 (3), 227–236.
- Toraño, J., Rivas, J.M., Rodríguez, R., Casal, M.M., 2003. Economic and technical results mining a 4 m thick coal seam in Spanish Carbonar colliery. *Glückauf* 139 (6), 323–328.
- Toraño, J., Rodríguez, R., Rivas, J.M., Pelegrí, A., 2004. Diminishing of the dust quantity during the management of granular material in a underground space. In: *Proceedings of XII International Conference on Modeling, Monitoring and Management of Air Pollution*, vol. 74, pp. 51–61.
- Toraño, J., Rodríguez, R., Diego, I., 2006a. Computational Fluid Dynamics (CFD) use in the simulation of the death end ventilation in tunnel and galleries. *Trans. Eng. Sci.* 52, 113–121.
- Toraño, J.A., Rodríguez, R., Diego, I., Rivas, J.M., Pelegrí, A., 2006b. Influence of the pile shape on wind erosion CFD emission simulation. *Appl. Math. Model.* 31, 2487–2502.
- Toraño, J., Torno, S., Menéndez, M., Gent, M.R., Velasco, J., 2009. Models of methane behaviour in auxiliary ventilation of underground coal mining. *Int. J. Coal Geol.* 80 (1), 35–43.
- Uchino, K., Inoue, M., 1997. Auxiliary ventilation at a heading face by a fan. In: *Proceeding of 6th International Mine Ventilation Congress*, pp. 493–496.
- Vinson, R., Volkwein, J., McWilliams, L., 2007. Determining the spatial variability of personal sampler inlet locations. *J. Occup. Environ. Hyg.* 4, 708–714.
- Wala, A., Jacob, J., Brown, J., Huang, G., 2003. New approaches to mine-face ventilation. *Miner. Eng.* 55 (3), 25–30.
- Zhang, Z., Chen, Q., 2006. Experimental measurements and numerical simulations of particle transport and distribution in ventilated rooms. *Atmos. Environ.* 40, 3396–3408.